Indian Journal of Chemical Technology
Vol. 29, September 2022, pp. 547-553
DOI: 10.56042/ijct.v29i5.62325

Enhanced photocatalytic degradation of azo dye using rare-earth metal doped TiO_2 under visible light irradiation

R Anisha* & E K Kirupa Vasam

Department of Chemistry & Research Centre, Nesamony Memorial Christian College, Marthandam, Tamilnadu 629 165, India

E-mail: anisharusselraj@gmail.com

Received 13 April 2022; accepted 6 July 2022

Lanthanum doped TiO_2 nanoparticles (La doped TiO_2) have been prepared by a sol-gel process using $TiO(C_4H_9)_4$ as raw material and are characterized using XRD, FT-IR, SEM-EDS, TEM and UV-DRS. The insertion of La ion in TiO_2 lattice has been confirmed by SEM-EDS and XRD data. TEM studies have confirmed that La ions are uniformly doped over TiO_2 lattice. The band gap level of La doped TiO_2 is decreased to 2.92 eV with a red shift due to charge transfer reaction which is confirmed by UV-DRS. The photocatalytic activities of the synthesized nanoparticles are evaluated for the degradation of Congo red dye (20 ppm) in an aqueous solution with La doped TiO_2 (0.25 g) at *p*H= 6.3, under solar light irradiation. The photocatalytic results confirmed that the La doped TiO_2 show good photocatalytic activity and can be considered as a promising photocatalyst for the degradation of organic pollutants in water. Due to the stability of La doped TiO_2 nanoparticles, it could be reused for more than five cycles reaching 100% degradation efficiency.

Keywords: Congo red, La doped TiO_2, Photocatalytic degradation, Sol-gel method, Visible light, remediation

Dye pollutants produced from various kinds of industries are becoming a major source of environmental contamination[1]. Dyes absorb the sunlight and reduce the photosynthetic capability of aquatic plants and microorganism. Many of these dyes are carcinogenic, mutagenic and genotoxic[2]. Treatment of waste water by physical and chemical methods has been applied in various studies[3,4]. These methods have some drawbacks such as high operational cost, complicated operational methods, releasing aromatic amines and formation ofby-products[5]. Simultaneously these methods are unable to remove the dye molecules completely and significant amount of sludge is formed which cause secondary pollution[6,7]. Recently there has been considerable interest in the utilization of advanced oxidation processes (AOP) for the complete degradation of dyes used in various industries. This process helps to convert the composition of organic dyes entirely into H_2O, CO2 and other non-toxic compounds without conveying other consequent pollution[8,9]. Photocatalytic treatments are based on in situ generation of highly reactive hydroxyl radicals. These radicals are highly oxidant species, and they attack most of the organic molecules. They are also characterized by low selectivity of attack which is a useful character for an oxidant used in waste water treatment. In the last decade, more attention has been given to TiO_2 due to its high photocatalytic activity, nontoxicity and high stability in aqueous solution[10]. Moreover, nanostructured TiO_2 often exhibit excellent photocatalytic activity, owing to their large specific area and good dispersion in aqueous solutions[11]. TiO_2 is generally considered to be the best photocatalyst and has the ability to detoxicate water from a number of organic pollutants[12]. In order to enhance the photocatalytic activity of TiO_2 catalysts many modification methods have been developed including doping other elements into TiO_2 photocatalyst. The photocatalytic activities were obviously enhanced in most cases[13-16]. The major doping methods include metal-photo depositing[17,18], metal ion-implantation[19], plasma CVD method[20,21], solgel process[22], hydrothermal method[23,24] and wet impregnation method[25]. Visible light induced photocatalytic activity of titania with rare-earth elements, like lanthanum, has attracted a lot of attention (Parida and Sahu, 2008)[26]. In this work, we have provided a simple route for synthesizing Lanthanum doped TiO_2 based on sol gel method. The purpose of the current work is to introduce a fast, economical and eco-friendly method for treating pollutants. Moreover, this study has investigated the photocatalytic degradation of Congo

red dye molecules using Lanthanam doped TiO_2 nanoparticles and their performance based on various characterization techniques. In this present study La doped TiO_2 photocatalyst with good light harvesting capacity was synthesized by a simple sol gel method followed by calcinations (Scheme 1).

Experimental Section

Preparation of La doped TiO_2particle

All chemicals and reagents were of analytical grade and used without further purification. Double distilled water was used all over the experiment.The Lanthanum doped TiO_2 photocatalyst was prepared by sol-gel method. Titanium (IV) is isopropoxide (TIP) acts as the precursor of titanium. TIP (15mL) was added drop wise to 30 mL of ethanol with constant stirring. To this, required amount of La $(NO_3)_3.6H_2O$ was added as lanthanum precursor, the resulting solution was allowed to aging for several hours to form a gel. The gel was dried at 80°C for 12 h and was calcined for 2 at the temperature of 450°C to form fine crystalline powder of the photocatalyst.

Characterization

The particle size and crystalline phase of the prepared photocatalyst were determined by powder XRD with Cukα radiation (λ=1.5406 A˚) as an incident beam in 2θ mode over a range of 20-80°C operated at 40 kV, and 30 mA. The presence of functional groups and the nature of photocatalyst were identified by (AVATAR 370) FT-IR technique using a Jasco FTIR-4600, Japan. The optical properties were investigated using DRS analysis (Agilent Cary 5000) with $BaSO_4$ as the reference material. The surface morphology along with its elemental composition was analyzed by SEM (FEI QuantaFEG200F) equipped with an Energy Dispersive X-ray (EDS) Spectrophotometer operated at 30kV and HR TEM, (JEOL-2100) with an accelerating voltage of 200kV and resolution point 0.194nm.

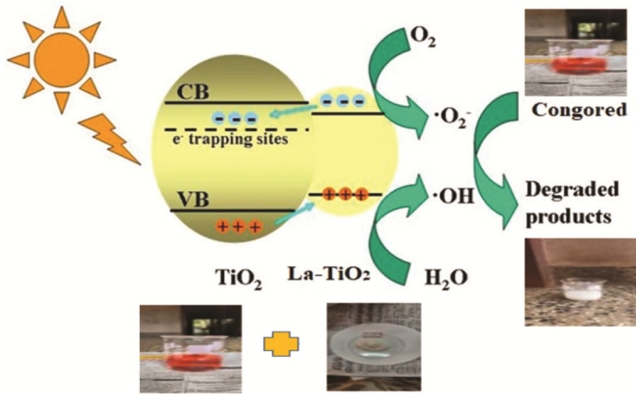

Scheme 1 —Pictorial depiction for the photocatalytic degradation of Congo red over La doped TiO_2 nanophotocatalyst under induced visible light.

Evaluation of photocatalytic activity

The La doped TiO_2 samples were tested for their photocatalytic activity by measuring its photodegradation with a pollutant dye, Congo red in aqueous solution under visible light at room temperature. Dye solution (100 mL) along with 250 mg of La doped TiO_2 nanoparticles were taken in a beaker which was magnetically stirred for 30 min in the dark to achieve a saturated adsorption desorption equilibrium between the photocatalyst and the dye molecules. Suspension of the Congo red (2 mL) was withdrawn and centrifuged for spectrophotometric analysisat λ_{max} = 500 nm, which corresponds to the maximum absorbance of the dye. The percentage of degradation was calculated by the formula,

$$\% \text{ Degradation} = (C_0\text{-}C_t)/C_0\times100 \quad \ldots (1)$$

Where, C_0 is represents initial concentration of Congo red dye, C_t is final concentration of Congo red dye after visible light irradiation.

Results and Discussion

XRD analysis

XRD characterization is an effective technique to determine crystal phase and size of materials. Figure 1 represents the XRD patterns of TiO_2 (1a) and la doped TiO_2 (1b). The XRD patterns of La doped TiO_2 exhibited diffraction peaks at 2θ of 25.2, 37.9, 47.9, 62.7 for anatase (JCPDS card, No.21-1272) 35, 36.There were no peaks for the formation of metal oxide such as La_2O_3 in La doped TiO_2. La^{3+}ion introduced into TiO_2 lattice, resulted in the formation of structural defects, which changed the band gap, by the extension of excitation energy from UV to visible region[27]. This enhancement of photo catalytic activity of La doped TiO_2 is due to the formation of two additional energy levels (4f & defect levels) that prevent the electron-hole recombination[28]. Furthermore, the phase of La element cannot be found in fig.1demonstrating that La^{3+} is successfully incorporated into the TiO_2 lattice. The average crystallite size of the samples was calculated by the Debye -Scherer formula.

$$D = K\lambda/\beta\cos\theta \quad \ldots (2)$$

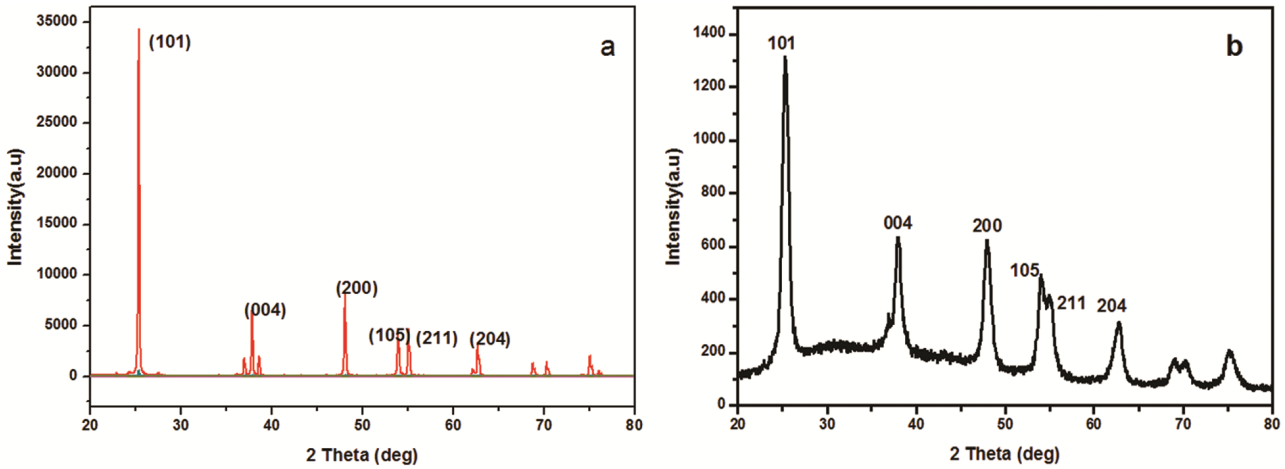

Fig.1 — Xrd patterns of (a) TiO_2 and (b) La doped TiO_2

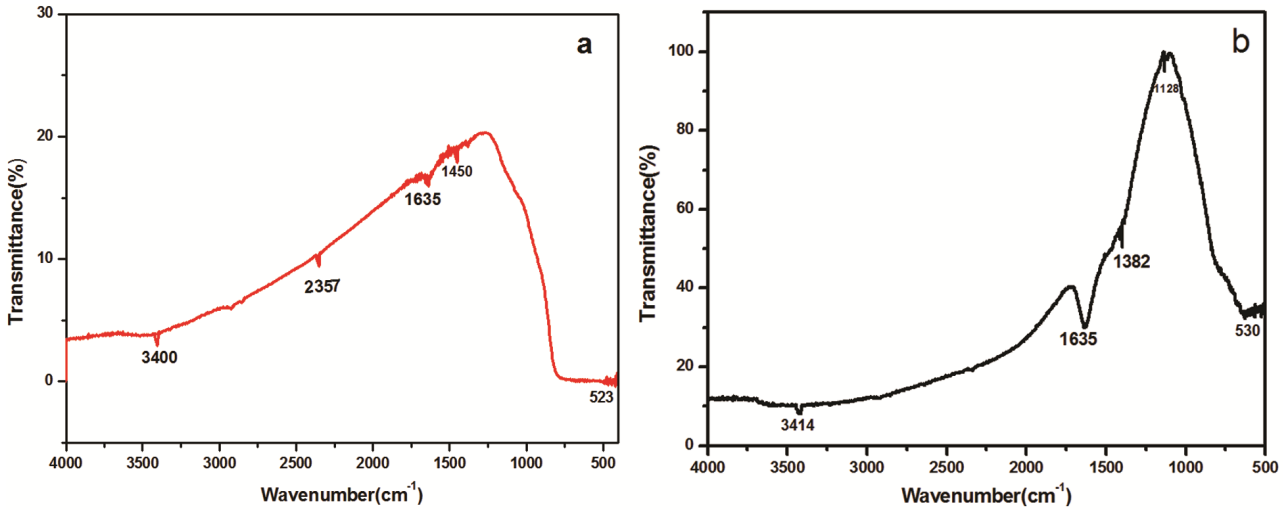

Fig. 2 —FT-IR spectra of (a) TiO_2 and (b) La doped TiO_2

where D represents the average crystalline size, 0.9 indicates the shape factor of grain, λ corresponds to wavelength of X-ray, β gives the FWHM of diffraction peak and θ is incident angle of X-ray. The average crystal size of the La doped $TiO_2$was calculated to be 10 nm.

FT-IR analysis

The FT-IR spectra of pure TiO_2 (2a) and La doped TiO_2 (2b) nanoparticles are shown in Fig. 2. The absorption bands at 3414 cm^{-1} and 1635 cm^{-1}, correspond to the stretching vibration modes of -OH bonds which represent that more number of water molecules are adsorbed on the lattice sites of La^{3+}-TO, therefore the generation of more $OH^{\bullet}$ during visible light irradiation is responsible for photocatalytic activity the nanoparticles.The characteristic band at 530cm^{-1} is due to the vibrational mode of Ti-O-La bond formation that shift the peak absorption to a low wave number which was reported asearlier[29].

Morphological analysis

The surface morphology and chemical composition of the prepared catalyst were studied by SEM and EDS analysis. Figure 3a shows SEM images of pure TiO_2 and Fig. (3b, 3c) shows the SEM images of La doped TiO_2.The SEM images of La-doped TiO_2 showed agglomerated particles with uneven size distribution and decreased particle size compared to undoped TiO_2.Moreover, the decreased particle size has increased the surface area to a considerable extent, which provides more photocatalytic sites for the catalytic degradation of organic contaminants[30].

Figure 4 shows the EDAX pattern of the La doped TiO_2 showed peaks corresponding to co-doped elements as 4:31:65 atomic % proportion of La: Ti: O

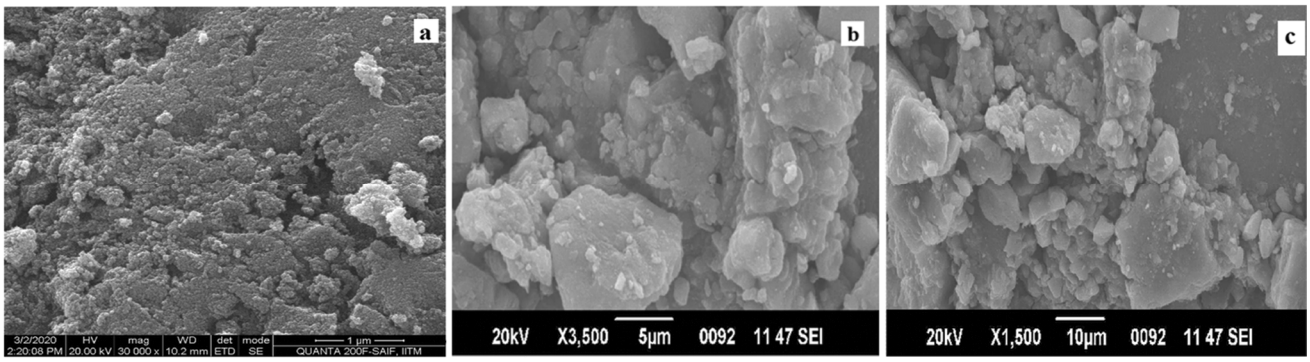

Fig. 3 — SEM images of (a) undoped TiO_2 and (b and c) La doped TiO_2

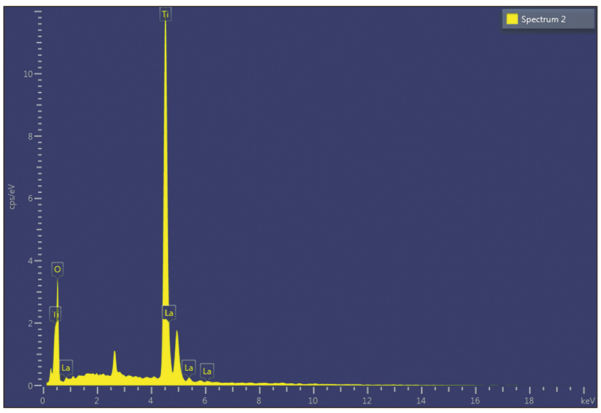

Element¤	Line Type¤	Wt%¤	Atomic %¤
O¤	K series¤	35.67¤	65.32¤
Ti¤	K series¤	50.34¤	30.94¤
La¤	L series¤	13.99¤	3.74¤
Total:¤	¤	100¤	100¤

Fig. 4 — EDAX spectrum of La doped TiO_2 nanoparticles

respectively, that confirmed the successful incorporation of 4% lanthanum into TiO_2 lattice

TEM analysis

Figure 5 (a, b, c & d) shows the HR-TEM images ofLa doped TiO_2.TEM images showed almost spherical shaped particles with uniform size distribution within the range 6-15 nm which is in good agreement with the crystallite size obtained from XRD pattern. A lattice spacing of 0.37 nm corresponded to anatase TiO_2 (101) crystal plane in Fig. 5 (d)[31,32] which is also the highest intense peak in XRD. The particle size distribution histogram obtained by Guassian fitting method shown in Fig. 5 (e) confirmed the average size of La doped TiO_2 as 10 nm which exerts the decreased particle size of TiO_2 due to co-doping of Lanthanum.

Optical absorption properties

The optical absorption property of La doped TiO_2 photocatalyst was investigated by UV-Vis DRS in the range 300-800 nm and the results are shown in Fig. 6 (a).The spectra of La doped TiO_2 showed a red shift dueto a charge-transfer process between the TiO_2 valence or conduction band and 4f level of La ion. Therefore, titania doped with La ion increased the absorption range in the visible-light region. Moreover, the band gap energies (E_g), which are estimated from the intercept of tangents to the plot of $(\alpha h\upsilon)^{1/2}$ versus photo energy were 2.92 eV as illustrated in Fig. 6(b). This extended absorbance indicated the possible enhancement in the photocatalytic activity of La doped TiO_2 by visible light.

Photocatalytic degradation studies

Figure 7 indicates the UV-visible absorption spectra of degraded Congo red dye over Lanthanum doped TiO_2.The nanophotocatalyst has simulated the absorption of sunlight over the wavelength range of 400-700 nm. Intially the aqueous solution of Congo red with photocatalyst has shown a maximum absorption of 500 nm. During the course of reaction, the intensity of the maxima has decreased gradually and finally disappeared after 60 min of duration. This confirmed the degradation of the Congo red by using La doped TiO_2 photocatalyst.

Photocatalytic degradation mechanism

The mechanism of TiO_2 photocatalysis involve the generation of an e^- -h^+ pairs when it is irradiated with light. This electron hole pair thus generated will

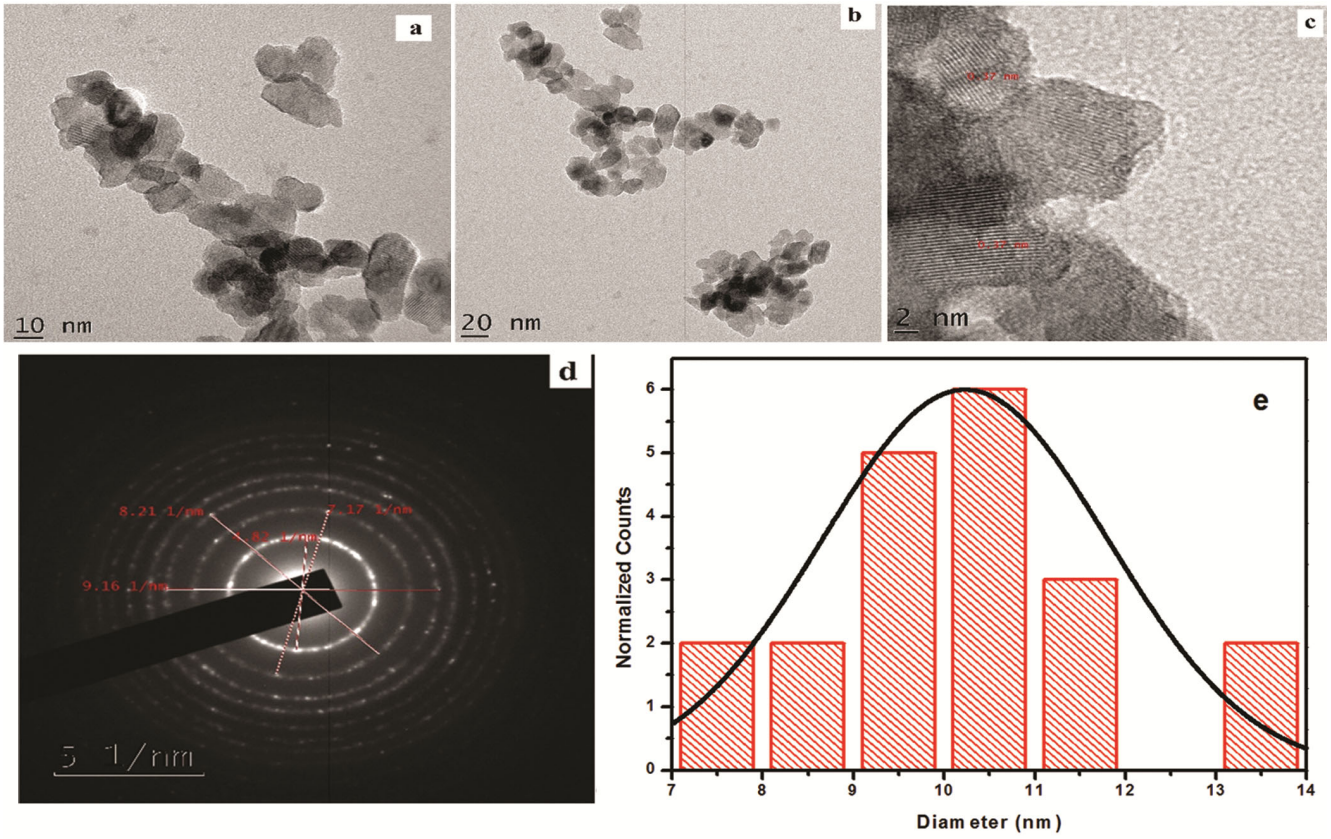

Fig.5 — (a and b) TEM images of La doped $Ti0_2$; (c) HRTEM images of La doped TiO_2; (d) SAED pattern of La doped TiO2 and (e)particle size distribution of La doped TiO_2

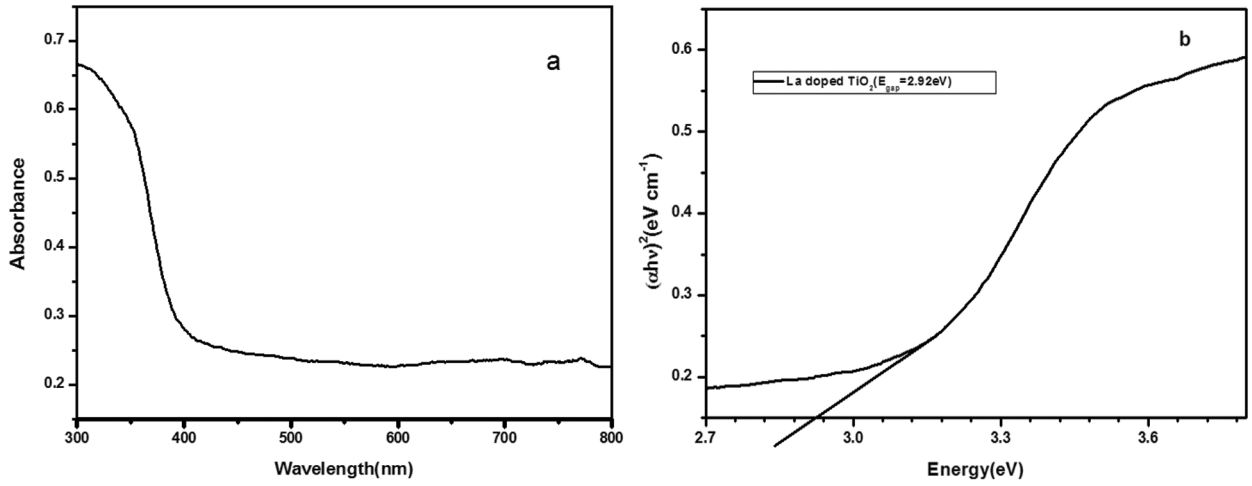

Fig.6. — (a) UV -Vis absorption spectra of La doped TiO_2 and (b) Optical band gap (Eg) spectra of La doped TiO_2

Overcome the electrostatic attraction between them and will tend to get separated and reach the surface by diffusion. Here the electrons are captured by O_2 and the hole is transferred to the adsorbed hydroxide to form hydroxide radicals ($OH^{\bullet}$). However, the TiO_2 photocatalytic system is inefficient due to a high chance of recombination of electron-hole pairs[33]. When rare earth ions like La, is doped with TiO_2 an electronic state is newly created between valence and conduction band, and thus band gap energy is reduced. This will enhance the absorption of sunlight and enhance the efficiency of the photocatalytic reactions (Fig. 8)

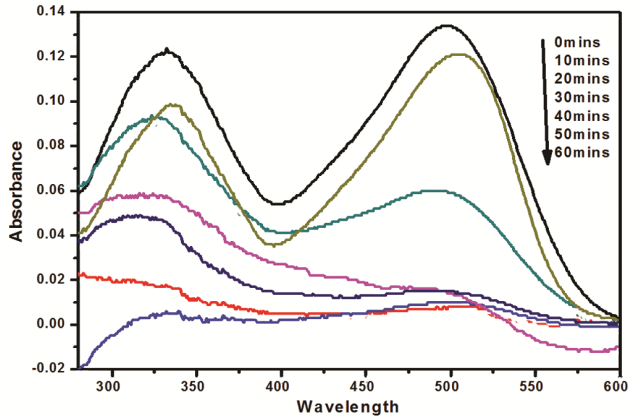

Fig. 7 — UV- Absorption spectra of dye under visible light by using la doped TiO2

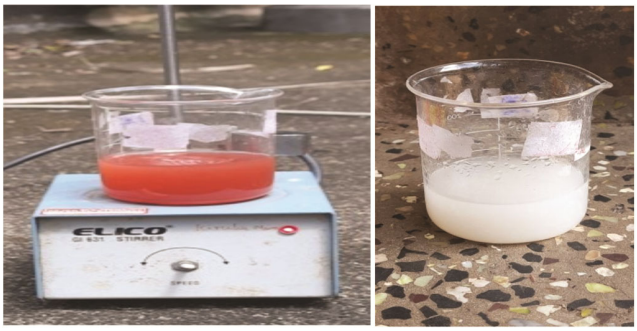

Fig. 8 — Visual observation of before and after degradation of dye

Total organic carbon (TOC) analysis

The degradation of Congo red with La doped TiO2 was analysed by a TOC analyser for different intervals of time from 0 min to 60 min duration. Initially, the TOC of Congo red and the photocatalyst was found to be 7560 mg/L and was reduced to 40.28 mg/L after 60 min of irradiation. This has confirmed the complete mineralization of Congo red by La doped TiO_2 nano photocatalyst. The outcomings obtained in this analysis has confirmed that La doped TiO_2 nano photocatalyst is responsible for the complete mineralization of the Congo red into a less complex product of water and carbon dioxide.

Estimation of chemical oxygen demand (COD) analysis

Photocatalytic degradation of Congo red was also confirmed by COD analysis before and after the experimental study, since it is an effective technique to measure the organic strength of waste water. The COD of the dye solution before (20155.2 mg/L) and after (92.43 mg/L) the treatment was estimated. The decrease in COD values of dye solution showed the complete mineralization of dye molecules along with the removal of colour.

Recycling ability of catalyst

Recycling ability of photocatalyst is required for large scale industrial application to degrade the contaminants. The photocatalyst was separated after the photocatalytic experiment from the photoreactor, it is washed several times with water to remove the adsorbed particles over it and dried at 100°C and its performance is analysed for several times. The reused photocatalyst showed good performance and stability. The degradation rate is almost unchanged for about five cycles and showed a loss of 10% for the sixth cycle indicating that the catalyst can be reused for more cycles. This performance has indicated an excellent long-term stability and good potentiality of the photocatalystfor waste water treatment applications.

Conclusion

La doped TiO_2nano photocatalyst was synthesized by sol-gel method followed by hydrothermal treatment. The structural, morphological and optical studies were investigated. The investigations made on the present study are:

In XRD, no additional peaks are formed forLa_2O_3 and hence La^{3+} ion introduced into TiO_2 lattice, resulted in the formation of structural defects with the formation of two additional energy levels (4f & defect levels) that prevent the electron-hole recombination.

IR spectra of La doped TiO_2 nanoparticles indicated that the adsorption of water molecules is more in the lattice sites of La^{3+}-TO, generating more $OH^{\bullet}$ during visible light irradiation and is responsible for the remarkable photocatalytic activity of the prepared catalyst.

SEM with EDAX analysis showed agglomerated particles with uneven size distribution and decreased particle size is responsible for the catalytic degradation of organic contaminants. It also confirmed the successful incorporation of 4% lanthanum into TiO_2 lattice.

TEM analysis showed almost spherical shaped particles, with a lattice spacing of 0.37 nm that corresponds to anatase TiO_2 (101) crystal plane. The average size of La doped $TiO_2$was estimated to be 10 nm.

In UV-Vis DRS analysis, the spectra of La doped TiO_2 showed a red shift due to a charge-transfer process. Moreover, the band gap energy (E_g) was 2.92 eV. This extended the absorbance of photocatalyst to visible region.

The TOC & COD analysis, confirmed the complete mineralization of the Congo red into a less complex product of water and carbon dioxide.

The reused photocatalyst showed good performance and stability. The degradation rate is almost unchanged for about four cycles and showed a loss of 10% for the fifth cycle indicating that the catalyst can be reused for some more cycles. This performance indicated that the photocatalyst has an excellent long-term stability and good potential for the treatment of waste water.

Finally, Congo red dye (20ppm), a model pollutant was degraded successfully with 0.25 g of photocatalyst, at *p*H 6.3. Thus, it can be concluded that doping TiO_2 with lanthanum is a good route to increase the degradation of emerging pollutants using visible light.

Conflicts of author

The authors declare there are no conflicts of interest.

References

1 Yingxuehen, Kangwang & Liping Lou, *J Photochem Photobiol A Chem*, 163 (2004) 281.
2 Mathur N, Bhatnagerp & Sharma P, *Univ J Environ Res Tech*, 2 (2012) 1.
3 Vajnhandl S, Le A & Marechal, *Dyes Pigm*, 65 (2005) 89.
4 Shu H Y & Chang M C, *J Hazard Mater*, B125 (2005) 96.
5 Kavita Pamecha, Vinod Mehta & Kabra B V, *Adv Appl Sci Res*, 7 (2016) 95.
6 Bouberka, Zohra, Benobbou Khalil A, Khenifi Alcha & Maschke Ulrich, *J Photochem Photobiol* A, 275 (2014) 21.
7 Esther Forgacs, Tibor Cserhati & Gyula Oros, *Environ Int*, 30 (2004) 953.
8 Azbar N, Yonar T & Kestioglub K, *Chemosphere*, 55 (2005) 35.
9 Chung-Hsin Wu, Chung-Liang Chang & Chao Yin Kuo, *Dye Pigm*, (2006) 187.
10 Hu C & Wang Y, *Chemosphere*, 39 (1999) 2107.
11 Tianjie Hong, Jun Mao, Feifei Taoand & Mingxuan Lan, *Molecules*, 22 (2017) 2044.
12 Kansal S K, Singh M & Sud D, *J Hazard Mater*, 141 (2007) 581.
13 Ihara T, Miyoshi M, Iriyama Y, Matsumoto O & Sugihara S, *Appl Catal B: Environ*, 42 (2003) 403.
14 Dana D, Vlasta B, Milan M & Malati M A, *Appl Catal B: Environ*, 37 (2002) 91.
15 Di P A, Garc L E & Iked S, *Catal Today*, 75 (2002) 87.
16 Hu C, Tang Y C & Tang H X, *Catal Today*, 90 (2004) 325.
17 Jin S & Shiraishi F, *Chem Eng J*, 97 (2004) 203.
18 Di P, Agatino G L & Elisa M G, *Appl Catal B: Environ*, 48 (2004) 223.
19 Yamashita H, Harada M & Misaka J, *Catal Today*, 84 (2003) 191.
20 Sugiyama K, Ogawa T & Saito N, *Surf Coat Technol*, 174 (2003) 882.
21 Awitor K O, Rafqah S, Geranton G, Sibaud Y, Larson P R, Bokawela R S P, Jernigen J D & Johnson M B, *J Photochem Photobiol A: Chem*, 199 (2008) 250.
22 Rampaul A, Parkin I P, O'Neill S A, Souza J D & Mills A, *Polyhedron*, 22 (2003) 35.
23 Stylidi M, Kendarides D I & Verykios X E, *Appl Catal B: Envirol*, 40 (2003) 271.
24 Liu H Y & Gao L, *J Amer Ceram Soc*, 87 (2004) 1582.
25 Houas A H, Laccheb M, Ksibi E, Elaloui C, Guillard & Herrmann J M, *Appl Catal B: Environ*, 31 (2001) 145.
26 Sanja J, Armakovic, Mirjana Grujic-Brojcin, Maja Scepanovic & Stevan Armakovic, *Arab J Chem*, 12 (2017) 5355.
27 Wu X H, Ding X B, Qin W, He W D & Jiang Z H, *J Mater*, 137 (2006) 192.
28 Zeinhom El-Bahy, Adel A Ismail & Reda A Mohamed, *J Hazard Mater*, 166 (2009) 138.
29 Putu Mahendra I, Adri Huda, Ha Minh Ngoc, Phan Trung Nghia, Tamrin Tamrin & Basuki Wirjosentono, Inv *Arab J Basic Appl Sci*, 26 (2019) 242.
30 Mukthar Ali S M Y M & Sandhya K Y, *RSC Adv*, 6 (2016) 60522.
31 Yermakov A Y, Zakharova G S, Uimin M A, Kuznetsov M V, Molochnikov L S, Konev S F, Konev A S, Minin A S, Mesilov V V, Galakhov V R, Volegov A S, Korolyov A V, Gubkin A F, Murzakayev A M, Svyazhin A D & Melanin K V, *J Phys Chem C*, 120 (2016) 28857.
32 Zhong-liang Shi, Hong Lai, Shu-hua Yao & Shao-Feng Wang, *Chinese J Chem Phys*, 25 (2012) 96.
33 Xie Y & Yuan C, *Appl Catal B: Environ*, 46 (2003) 251.